



ELSEVIER

Journal of Magnetism and Magnetic Materials 163 (1996) 184–192



New dense Kondo systems $Ce_3Pd_{20}Ge(Si)_6$ and related compounds $Sm(Yb)_3Pd_{20}Ge(Si)_6$

V.N. Nikiforov^{*}, Yu.A. Koksharov, J. Mirković, Yu.V. Kochetkov

Low Temperature Department, Faculty of Physics, M.V. Lomonosov State University, 119899 Moscow, Russia

Received 26 January 1995; revised 4 January 1996

Abstract

The electrical and magnetic properties of a new cubic system $Ln_3Pd_{20}X_6$ ($Ln = Ce, Sm, Yb$; $X = Si, Ge$) have been studied. The electrical resistivity ρ versus temperature shows a minimum at ~ 50 K for $Ce_3Pd_{20}Si_6$, and at ~ 10 K for $Ce_3Pd_{20}Ge_6$. Below these temperatures $\rho(T)$ follows a logarithmic law down to 4.2 K. In $Ce_3Pd_{20}Si_6$ the thermal behavior of the magnetic moment displays an antiferromagnetic anomaly at approximately 50–60 K and marked ‘superparamagnetic’ properties on further cooling. To explain the unusual magnetic behavior of $Ce_3Pd_{20}Si_6$ a model of ‘molecular’ magnetism is suggested for one of two cerium sublattices. Another cerium subsystem is likely to respond for Kondo anomalies. In contrast with cerium compounds, the samarium and ytterbium homologues display normal metallic behavior with a nonmagnetic ground state down to 4.2 K.

Keywords: Rare-earth compounds; Kondo effect; Crystal field effect; Static magnetic properties; Superparamagnetism

1. Introduction

Dense Kondo systems (DKS) have attracted much attention in connection with their unusual magnetic, heavy-fermion, superconducting and other properties. Much experimental and theoretical work has been done on these subjects. The most important problem in the physics of DKS is the nature of the ground state. The competition between magnetic and Kondo interactions was traditionally considered to result in either a magnetic ground state with significant full suppression of Kondo features, or in a nonmagnetic Kondo ground state [1]. However, in the last decade it has been found that there are many

f-electron compounds in which magnetic ordering coexists with Kondo anomalies [2]. Examples include the antiferromagnetics $UAgCu_4$, U_2Zn_{17} , UCd_{11} , $CeAl_2$, CeB_6 and $CeAgGe_6$, and the ferromagnetics $CeRhB_6$, $CeSi_x$ ($x < 1.85$), $CeGe_{2-x}Si_x$, $Ce_xLa_{1-x}Ge_2$ and Ce_4Bi_3 [2]; these materials are known as ‘Kondo magnetics’. Experimental evidence for a ‘Kondo magnetic’ compound includes Kondo-like thermal behavior of the electrical resistivity, a reduced value of magnetic entropy at the magnetic transition point, and a very small ordering magnetic moment compared with that calculated from the high-temperature Curie constant.

Many nonmagnetic DKS seem to be close to magnetic ordering [2] because they can undergo a magnetic transition either under pressure, e.g. UB_{13} [3], or after a minor change in composition, e.g.

^{*} Corresponding author. Fax: +7-095-932-8876, +7-095-276-2135; email: nvn@hohlov.msk.su; nvn@lt.phys.msu.su.

CeSi_x [4]. From this point of view, the recently synthesized [5] system Ce₃Pd₂₀X₆ (X = Si, Ge) and related compounds Ln₃Pd₂₀Si₆ with Ln = Sm, Yb offer the promise of convenient subjects for study. These compounds have a cubic structure which is only little affected by the replacement of Ln or X atoms. Besides, the Ce atoms occupy two non-equivalent positions with different local environments. In this case, the coexistence of different kinds of ground state (e.g. Kondo and magnetic) can be expected, as has been reported for Ce₅Rh₄ [6].

This paper describes detailed experimental studies of some of the magnetic and transport properties of Ln₃Pd₂₀X₆, with Ln = Ce, Sm, Yb and X = Si, Ge. Preliminary results were presented at SCTE-11 (Wroclaw, 1994) [7].

2. Experimental details

Polycrystalline samples of Ln₃Pd₂₀X₆ compounds were prepared using a melting technique in an arc furnace in an argon atmosphere followed by long-term annealing [5]. The crystal structures of these compounds were determined by diffraction measurements [5]. X-ray analysis confirmed the absence of any additional phases within experimental accuracy (5%).

The electrical resistivity was measured in the temperature range 4.2–200 K by a conventional dc four-probe technique using a Solartron 7081 precision voltmeter. Spot-welded copper contacts were used. The sample temperature was controlled by a germanium thermometer to an accuracy of 0.1 K.

The static magnetic moments $M(T)$ were measured using a vibrating sample magnetometer PARC-M-155 at temperatures 4.2–200 K and in magnetic fields up to 7000 Oe. The lowest measurable magnetic moment was 10⁻⁵ emu.

3. Results

3.1. Electrical resistivity

Fig. 1 shows the temperature dependence of the electrical resistivity $\rho(T)$ for Ce₃Pd₂₀Ge₆ and Ce₃Pd₂₀Si₆. The variation in ρ versus T for Ce₃Pd₂₀Si₆ exhibits a broad minimum at the temper-

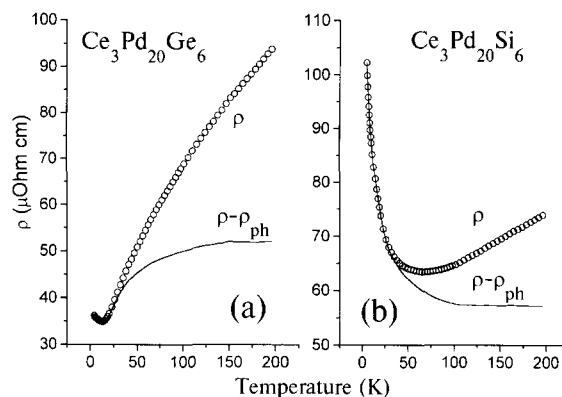


Fig. 1. Temperature dependence of the dc electrical resistivity for Ce₃Pd₂₀Ge₆ (a) and Ce₃Pd₂₀Si₆ (b). Solid lines: the 'magnetic' contribution to the resistivity ρ after subtracting the phonon contribution.

ature $T_{\text{min}} \approx 50$ K. Below T_{min} down to 4.2 K the resistivity gradually increases. A similar thermal behavior of the resistivity was found for Ce₃Pd₂₀Ge₆. However, in the latter compound $\rho(T)$ shows a minimum at $T_{\text{min}} \approx 10$ K. It is important to note that below the corresponding T_{min} the thermal variation of the resistivity can be well approximated by a logarithmic law [8]. This temperature behavior of the resistivity indicates the possibility of the Kondo effect in Ce₃Pd₂₀Si₆ and Ce₃Pd₂₀Ge₆.

At high temperatures the resistivity versus temperature $\rho(T)$ increases more linearly in Ce₃Pd₂₀Si₆ than in Ce₃Pd₂₀Ge₆. Moreover, in the latter compound the $\rho(T)$ curve takes a shape of an arc in the temperature range 25–200 K (Fig. 1).

For Ce compounds the phonon contribution ρ_{ph} was subtracted from $\rho(T)$ by means of the procedure described in Ref. [9]. To do this, the Debye temperatures T_{D} for the Ce₃Pd₂₀X₆ (X = Si, Ge) compounds were estimated using Lindemann's formula [10]:

$$T_{\text{D}} \approx B \sqrt{T_{\text{M}}} D_0^{1/3} A^{-5/6}, \quad (1)$$

where T_{M} is the melting temperature, D_0 is the mass density, A is the average atomic weight, and $B \approx 120$ is a numerical factor. The parameters and calculated values of T_{D} required for the estimation (1) are presented in Table 1.

The solid lines in Fig. 1 represent the electrical resistivity versus temperature after the subtraction of

Table 1

Lattice parameter a , mass density D_0 , melting temperature T_M [5] and Debye temperature T_D (Eq. (1)) for $Ce_3Pd_{20}Ge_6$ and $Ce_3Pd_{20}Si_6$

Compound	a (Å)	D_0 (g/cm ³)	T_M (K)	T_D (K)	T_{min} (K)
$Ce_3Pd_{20}Ge_6$	12.4453(4)	10.281(1)	1463	189	~ 10
$Ce_3Pd_{20}Si_6$	12.161(1)	10.03(2)	1553	211	~ 50

the phonon contribution. Note that in $Ce_3Pd_{20}Si_6$, the difference $\Delta\rho = \rho - \rho_{ph}$ is independent of temperature above T_{min} , while in $Ce_3Pd_{20}Ge_6$ $\Delta\rho$ demonstrates strong thermal variation. The characteristic arc shape of $\Delta\rho(T)$ suggests marked crystal field splitting [11,12].

In the $Sm_3Pd_{20}Si_6$ and $Yb_3Pd_{20}Si_6$ compounds the resistivity falls monotonically with decreasing temperature down to 4.2 K (Fig. 2). No anomalies were observed, except for a minor curvature in the $\rho(T)$ curve for $Sm_3Pd_{20}Si_6$ in the temperature range 25–200 K.

3.2. Magnetic measurements

Fig. 3 shows the temperature dependence of the static molar magnetic moment $M(T)$ of the $Ce_3Pd_{20}Ge(Si)_6$ compounds. The data correspond to an applied magnetic field $H_a = 500$ Oe. In $Ce_3Pd_{20}Ge_6$ the magnetic moment versus T demonstrates modified Curie–Weiss behavior at all temperatures. The Curie constant C , the Weiss constant θ and the temperature-independent susceptibility χ_0 were estimated in order to obtain the best fit to the

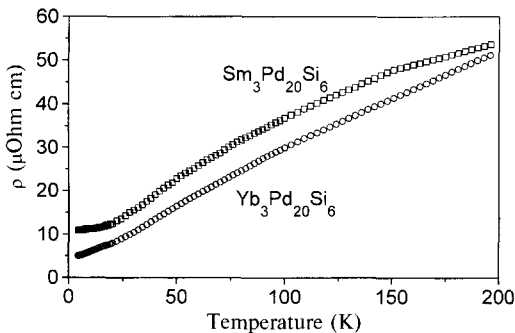


Fig. 2. Temperature dependence of the dc electrical resistivity for $Sm_3Pd_{20}Si_6$ and $Yb_3Pd_{20}Si_6$ compounds.

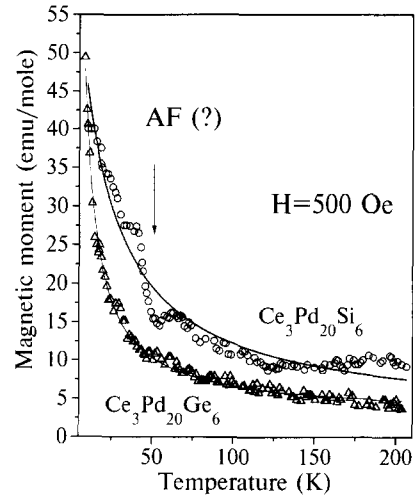


Fig. 3. Temperature dependence of the static molar magnetic moment for $Ce_3Pd_{20}Si_6$ and $Ce_3Pd_{20}Ge_6$ compounds with $H_a = 500$ Oe. Solid lines: results of the modified Curie–Weiss law fitting (see text).

measured data using the formula for the modified Curie–Weiss law:

$$\chi = \frac{M}{H} = \chi_0 + \frac{C}{T - \theta} \quad (2)$$

The effective magnetic moment μ_{eff} was calculated from the Curie constant C as follows

$$\mu_{eff} = \sqrt{\frac{3k_B}{N}} C, \quad (3)$$

where $N = 3 \times N_A$ is the number of Ce atoms per mole in $Ce_3Pd_{20}Ge(Si)_6$. The results of this fitting procedure are shown in Table 2. The reduced value of μ_{eff} may indicate a more significant CEF splitting of Ce^{3+} in $Ce_3Pd_{20}Ge_6$ in comparison with that in $Ce_3Pd_{20}Si_6$.

The thermal variation of the magnetic moment of $Ce_3Pd_{20}Si_6$ can be assimilated to the Curie–Weiss law only at high temperatures $T > 100$ K (Fig. 3). Near 60 K the $M(T)$ curve exhibits a pronounced anomaly characteristic of magnetic ordering. The existence of the magnetic transition in $Ce_3Pd_{20}Si_6$ is also confirmed by the unusual field dependence of the magnetic moment. In the case of $H_a = 500$ Oe, at all temperatures the magnetic moment of $Ce_3Pd_{20}Si_6$ is much higher than that of $Ce_3Pd_{20}Ge_6$. Fig. 4 shows the temperature dependence $M(T)$ for the

Table 2

Curie constant C , Weiss constant θ , the temperature-independent susceptibility χ_0 , and the effective magnetic moment μ_{eff} at various applied magnetic fields H_a

Compound	H_a (Oe)	C ($\text{cm}^3 \cdot \text{K}/\text{mol}$)	θ (K)	χ_0 (cm^3/mol)	μ_{eff} ($\mu_B/\text{Ce atom}$)
$\text{Ce}_3\text{Pd}_{20}\text{Ge}_6$	500	0.7	1	53×10^{-4}	1.5
$\text{Ce}_3\text{Pd}_{20}\text{Ge}_6$	4000	1.0	3	53×10^{-4}	1.6
$\text{Ce}_3\text{Pd}_{20}\text{Si}_6$	500	1.5	-6	91×10^{-4}	2.0

$\text{Ce}_3\text{Pd}_{20}\text{Ge}(\text{Si})_6$ compounds at $H_a = 4000$ Oe. Below ~ 50 K the magnetic moment of $\text{Ce}_3\text{Pd}_{20}\text{Si}_6$ is clearly less than that of $\text{Ce}_3\text{Pd}_{20}\text{Ge}_6$. With an increase in H_a from 500 to 4000 Oe leads to a drastic fall in the magnetic susceptibility of $\text{Ce}_3\text{Pd}_{20}\text{Si}_6$ below ~ 50 K, whereas the $M(T)$ curves for $\text{Ce}_3\text{Pd}_{20}\text{Ge}_6$ do not demonstrate an evident field dependence (Figs. 3 and 4, Table 2).

Fig. 5 shows the magnetic moment versus applied magnetic field for $\text{Ce}_3\text{Pd}_{20}\text{X}_6$ ($X = \text{Ge}, \text{Si}$) at various temperatures. The $M(H)$ curves for $\text{Ce}_3\text{Pd}_{20}\text{Ge}_6$ are linear at all temperatures. In contrast, there is a marked transformation from very nonlinear to linear behavior of $M(H)$ near 60 K in $\text{Ce}_3\text{Pd}_{20}\text{Si}_6$. Thus, both the temperature and field dependence of the magnetic moment indicate a transition to a magnetically ordered state in $\text{Ce}_3\text{Pd}_{20}\text{Si}_6$ at about 50–60 K. In the following we discuss the nature of this transition.

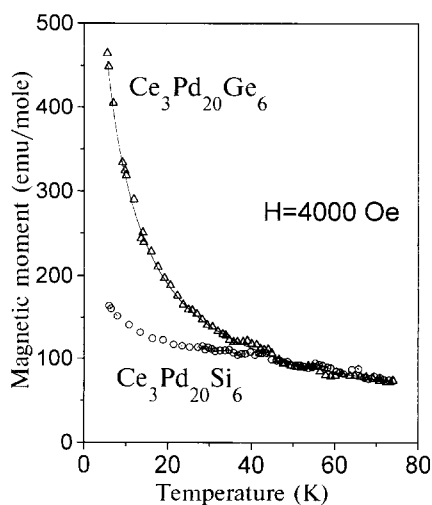


Fig. 4. Temperature dependence of the static molar magnetic moment for $\text{Ce}_3\text{Pd}_{20}\text{Si}_6$ and $\text{Ce}_3\text{Pd}_{20}\text{Ge}_6$ compounds with $H_a = 4000$ Oe. Solid line: results of the modified Curie–Weiss law fitting (see text).

3.3. Model of ‘molecular’ magnetism in $\text{Ce}_3\text{Pd}_{20}\text{Si}_6$

The magnetic transition in $\text{Ce}_3\text{Pd}_{20}\text{Si}_6$ does not seem to be of ferromagnetic type. First, the total molar magnetic moment below the anomaly temperature ~ 50 – 60 K is too small in comparison with the paramagnetic state (Figs. 3–5). Second, the field H_1 at which the magnetization $M(H)$ curves becomes linear is too high for ferromagnetics. Indeed, it can be seen from Fig. 5(b) that $H_1 \approx 1500$ – 2000 Oe. As a rule, in isotropic ferromagnetics the linear increase in the magnetic moment starts at fields of about 10^2 Oe [13]. On the other hand, the magnetization behavior of $\text{Ce}_3\text{Pd}_{20}\text{Si}_6$ is untypical of antiferromagnetics, since they are characterized by a linear $M(H)$ dependence up to quite high fields ($\geq 5 \times 10^3$ Oe) [14].

Similar behavior of the magnetic moment versus both T and H , has been observed in antiferromagnetic semiconductors $\text{EuTe}(\text{Se})$ [15], as well as in γ - FeCrNi alloys [16]. These materials, which on the whole are characterized by antiferromagnetic ordering, contain small ferromagnetic regions with large total effective magnetic moments ($> 40 \mu_B$). A marked feature of these ‘mixed antiferro–ferromagnetic’ compounds is the paramagnetic-like behavior of the magnetization, characterized by a relatively low magnetic saturation field (~ 1500 – 2000 Oe). Such behavior can be explained [17] within the model of noninteracting paramagnetic centers with the effective magnetic moment greatly exceeding that for single ions. This peculiarity has become known as the phenomenon of ‘superparamagnetism’ [18,19]. In γ - FeCrNi , ferromagnetic regions are clusters rich in Ni atoms, and in $\text{EuTe}(\text{Se})$ these are the sites of an auto-localization of conduction electrons.

There is one evident difference between the magnetic behavior described in Refs. [15,16] and in our work. In the former, the antiferromagnetic and ferro-

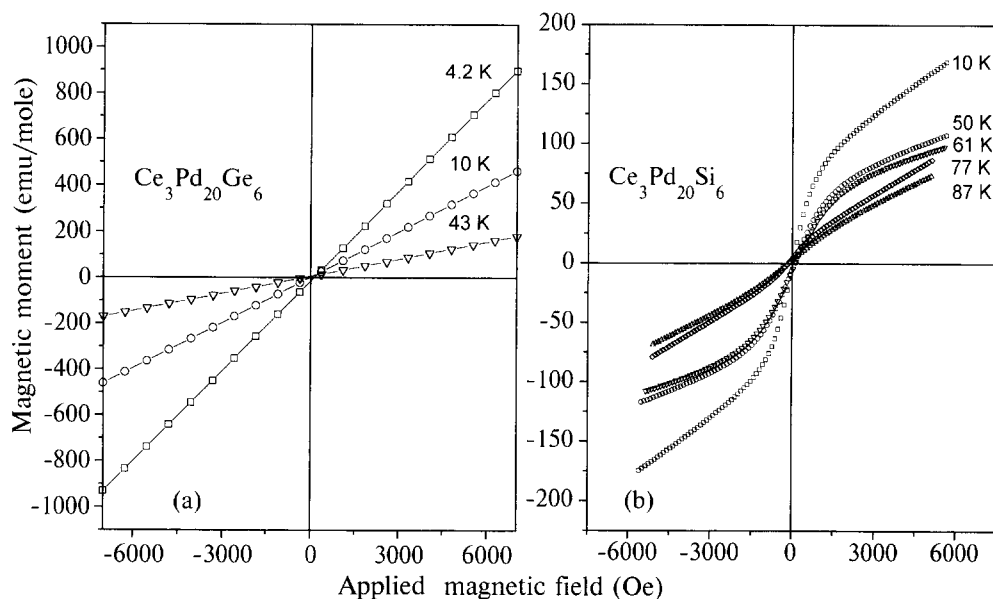


Fig. 5. Magnetization curves for $\text{Ce}_3\text{Pd}_{20}\text{Ge}_6$ (a) and $\text{Ce}_3\text{Pd}_{20}\text{Si}_6$ (b) compounds at various temperatures.

magnetic transitions occurred at markedly different temperatures T_{AF} and T_{F} , respectively. For example, in EuTe the characteristic temperatures were $T_{\text{AF}} = 7$ K and $T_{\text{F}} = 40$ K, so that the antiferro- and ferromagnetism in these systems seem to be quite independent. In $\text{Ce}_3\text{Pd}_{20}\text{Si}_6$, in contrast, the temperatures of the anomaly in $M(T)$ and the occurrence of nonlinearity of $M(H)$ are very close. This indicates that this antiferromagnetic ordering is related to the formation of 'superparamagnetic units'.

Is there anything in the crystal structure of $\text{Ce}_3\text{Pd}_{20}\text{Si}_6$ that could assume the role of some 'superparamagnetic unit'? The crystal structure of $\text{Ce}_3\text{Pd}_{20}\text{Ge}(\text{Si})_6$ can be considered as a superstructure of Cr_{23}C_6 [5]. Both compounds belong to the cubic system corresponding to space group $\text{Fm}\bar{3}\text{m}$. The projection of the $\text{Ce}_3\text{Pd}_{20}\text{Ge}(\text{Si})_6$ structure onto the ab plane is shown in Fig. 6. Only the cerium positions are shown because the total number of atoms per unit cell is quite large (116). The sites of Ce1 form a face-centered 'large' cube with other atoms of the cell inside. Eight atoms of Ce2 make up a 'small' cube with only Pd atoms inside. The coordination polyhedra of the Ce1 atoms consist of 12 Pd atoms in the case of $\text{Ce}_3\text{Pd}_{20}\text{Ge}_6$, and include six additional nearest Si atoms in the $\text{Ce}_3\text{Pd}_{20}\text{Si}_6$

crystal structure. The Ce2 coordination polyhedra, including 16 Pd atoms, are identical in both compounds.

A careful look at Fig. 6 allows us to select a 'small' cube of eight Ce2 atoms as a possible candidate for the 'superparamagnetic unit'. If the magnetic interactions between eight ions inside this cube are strongest, it could be considered as a 'molecule'

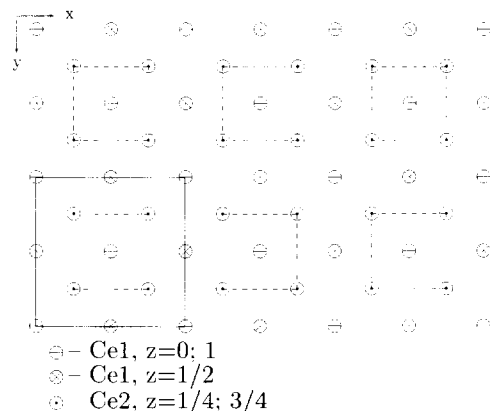


Fig. 6. Projection of $\text{Ce}_3\text{Pd}_{20}\text{Ge}_6$ crystal structure onto the ab plane. Only the Ce positions [5] are shown. Solid line: boundary of the unit cell; dashed lines: 'small' Ce2 cubes inside 'large' Ce1 cubes.

with an effective magnetic moment that increases on cooling. In the following we examine a model of such ‘molecule’.

There is a group of n equivalent localized magnetic moments $\mu = \mu_B g s$, where g is the Landé factor, μ_B is the Bohr magneton, and n is an even number. These spins are bound by isotropic ex-

change interactions and placed in the external magnetic field H_0 . The Hamiltonian of the system is

$$\hat{H} = \hat{H}_z + \hat{H}_{ex}, \tag{4}$$

where

$$\hat{H}_{ex} = - \sum_{\substack{l=1, m=1 \\ l \neq m}}^n A s_l s_m, \quad \hat{H}_z = - \sum_{i=1}^n \mu_B g s_i H_0. \tag{5}$$

If $\hat{H}_z \ll \hat{H}_{ex}$, the perturbation theory can be applied. It is clear that in the case of a positive exchange constant A ($A > 0$, ferromagnetic case), the ground level of this system corresponds to a maximum total spin

$$S_{tot} = s_1 + s_2 + \dots + s_{n-1} + s_n, \quad S_{tot(max)} = n \cdot s. \tag{6}$$

Indeed, \hat{H}_{ex} can be transformed to

$$\begin{aligned} \hat{H}_{ex} &= - \frac{A}{2} \sum_{i=1}^n [S_{tot}^2 - s_1^2 - s_2^2 - \dots - s_{n-1}^2 - s_n^2] \\ &= - \frac{A}{2} [S_{tot}(S_{tot} + 1) - ns(s + 1)]. \end{aligned} \tag{7}$$

The steady states of Eq. (7) may be characterized by the value of the total spin number S_{tot} only. The corresponding energies of these states are

$$E_s = - \frac{A}{2} S_{tot}(S_{tot} + 1), \quad S_{tot} = 0, 1, \dots, ns. \tag{8}$$

Fig. 7 shows schemes of the energy levels (8) with $n = 8$, $s = 5/2$ and $s = 1/2$. Since there are $k(S_{tot})$ states with the same value of S_{tot} , each energy level is $k(S_{tot}) \cdot (2S_{tot} + 1)$ -fold degenerate, where $k(S_{tot})$ is shown in Fig. 7. These values of $k(S_{tot})$ were calculated using the well known quantum mechanical rules for the addition of angular momentum vectors [20]. The magnetic moment of the system is

$$\langle M \rangle = \frac{\sum_{S=0}^{ns} k(S) e^{-E_s/k_B T} \sum_{j=-S}^S j e^{j \mu_B g H_0 / k_B T}}{\sum_{S=0}^{ns} k(S) e^{-E_s/k_B T} \sum_{j=-S}^S e^{j \mu_B g H_0 / k_B T}}. \tag{9}$$

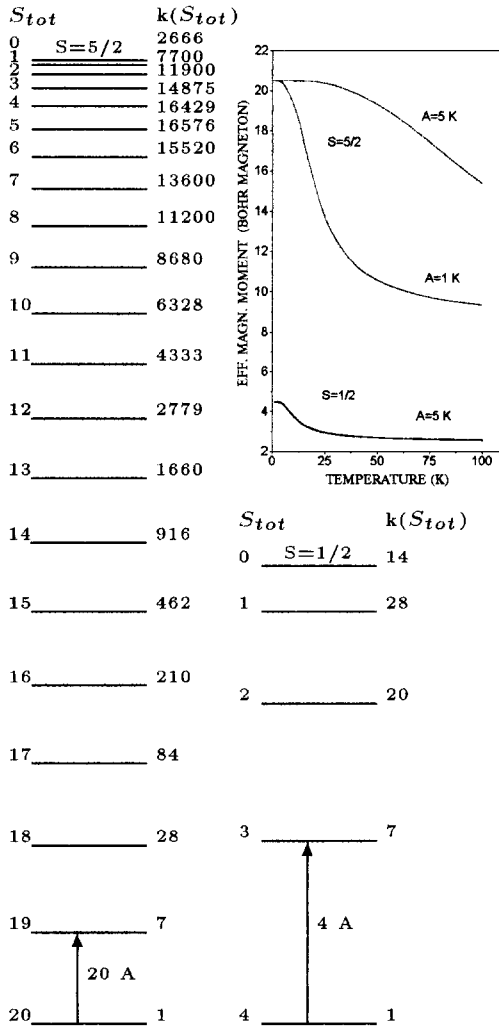


Fig. 7. Schemes of energy levels (in relative units) for the model of a magnetic ‘molecule’, formed by n spins s linked by isotropic exchange interactions ($n = 8$, $s = 5/2$ and $s = 1/2$). Inset: temperature dependence of the effective magnetic moment (Eqs. (3), (8) and (9)) for different values of s and the exchange interaction constant A .

In the case when only the ground level with $S_{\text{tot}} = ns$ is occupied, Eq. (9) can be reduced to

$$\langle M \rangle = \frac{\mu_B g \sum_{j=-ns}^{ns} j e^{j \mu_B g H_0 / k_B T}}{\sum_{j=-ns}^{ns} e^{j \mu_B g H_0 / k_B T}} = \mu_B g n s B_{n s} \left(\frac{n s g \mu_B H_0}{k_B T} \right), \quad (10)$$

where $B_j(x)$ is the Brillouin function [21]

$$B_j(x) = \frac{2j+1}{2j} \coth\left(\frac{2j+1}{2j}x\right) - \frac{1}{2j} \coth\left(\frac{x}{2j}\right).$$

If $x \ll 1$ then $B_j(x) = [(j+1)/3j]x$ and

$$\langle M \rangle = \mu_B^2 g^2 \frac{ns(ns+1)H_0}{3k_B T}. \quad (11)$$

Hence, the effective magnetic moment of our ‘molecule’ in the case of $n=8$, $s=5/2$ can reach a maximum value of $\mu_B \sqrt{ns(ns+1)} \approx 20 \mu_B$ (Fig. 7, inset). In the case of strong CEF splitting, the value $s=1/2$ should be used in Eqs. (8)–(11), and the maximum effective moment of the ‘molecule’ is much less (Fig. 7, inset). Probably, such situation occurs in $\text{Ce}_3\text{Pd}_{20}\text{Ge}_6$, where no ‘superparamagnetic’ phenomena is observed down to 4.2 K.

The above model has evident restrictions. The Hamiltonian (5) is probably too simple to be directly applicable to the real structure of $\text{Ce}_3\text{Pd}_{20}\text{Si}_6$. Allowance must be made for possible contributions to the magnetic moment from the delocalized magnetic moments, especially since Pd is known as a metal with unique enhanced ability of magnetic polarization [22]. Also, mean-field effects should be taken into account when examining the magnetization process in the ordered state. Nevertheless, the above model provides a way to explain the unusual magnetic behavior of $\text{Ce}_3\text{Pd}_{20}\text{Si}_6$.

In this connection, the question of a possible impurity phase may also arise. The low-field anomaly could be due to a trace amount of ferromagnetic impurity phase, although this can not explain the decrease in the magnetic susceptibility below 50–60 K. Therefore, an intrinsic antiferromagnetic

transition in $\text{Ce}_3\text{Pd}_{20}\text{Si}_6$ can be considered as most probable. It is unlikely that a ferromagnetic transition in an impurity phase and intrinsic antiferromagnetic ordering in $\text{Ce}_3\text{Pd}_{20}\text{Si}_6$ could take place at exactly the same temperature.

3.4. Crystal field calculations

Although unusual magnetic ordering was observed in $\text{Ce}_3\text{Pd}_{20}\text{Si}_6$ below about 50 K, in $\text{Ce}_3\text{Pd}_{20}\text{Ge}_6$ the low-temperature behavior of the reciprocal magnetic susceptibility (Fig. 8), as well as the marked reduction in the effective magnetic moment (Table 2) indicate the strong crystal electric field (CEF) splitting in this compound. The well known CEF Hamiltonian

$$H_{\text{CEF}} = \sum_{n,m} B_n^m O_n^m \quad (12)$$

for cubic symmetry can be reduced to

$$H_{\text{CEF}} = B_0^4 (O_4^0 + 5 \cdot O_4^4), \quad (13)$$

where B_n^m are the CEF parameters, O_n^m are the Stevens operators [23]. The Ce^{3+} ground term $^2F_{5/2}$ will be split by Eq. (13) into the doublet $\Gamma_7(\varphi_{1,2})$

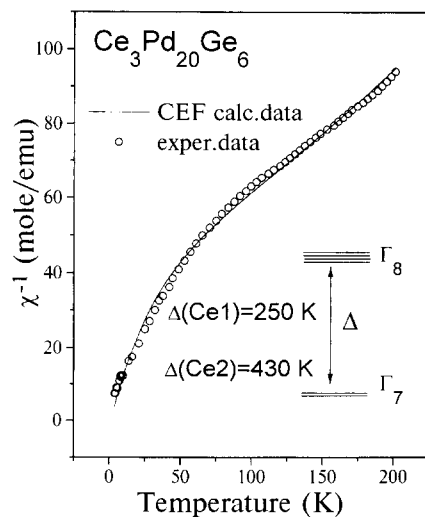


Fig. 8. Temperature dependence of the reciprocal magnetic susceptibility for $\text{Ce}_3\text{Pd}_{20}\text{Ge}_6$ ($H_a = 4000$ Oe). Solid lines: results of the CEF calculation (see text).

and the quartet $\Gamma_8(\varphi_{3-6})$ [24], with the following wave functions φ_i :

$$\varphi_1 = -0.41 \left\langle -\frac{5}{2} \right\rangle + 0.91 \left\langle \frac{3}{2} \right\rangle,$$

$$\varphi_2 = 0.91 \left\langle -\frac{3}{2} \right\rangle - 0.41 \left\langle \frac{5}{2} \right\rangle,$$

$$\varphi_3 = \left\langle \frac{1}{2} \right\rangle, \quad \varphi_4 = \left\langle -\frac{1}{2} \right\rangle,$$

$$\varphi_5 = 0.41 \left\langle -\frac{3}{2} \right\rangle + 0.91 \left\langle \frac{5}{2} \right\rangle,$$

$$\varphi_6 = 0.91 \left\langle -\frac{5}{2} \right\rangle + 0.41 \left\langle \frac{3}{2} \right\rangle,$$

where $\langle z |$ is the eigenfunction of the operator \hat{J}_z for the total angular momentum.

To calculate the CEF paramagnetic susceptibility Van Vleck formulae [25] should be used:

$$\chi_{\text{CEF}}^{(z)} = \frac{N_A}{k_B T \cdot Z} \sum_n |(n|M_z|n)|^2 \exp\left(-\frac{E_n}{k_B T}\right) + \frac{2N_A}{Z} \sum_{n' \neq n} \frac{|(n|M_z|n')|^2}{E_{n'} - E_n} \exp\left(-\frac{E_n}{k_B T}\right), \quad (14)$$

where N_A is Avogadro's constant, k_B is Boltzmann's constant, E_n is the energy of the n th CEF eigenfunction in the absence of an external magnetic field, $\hat{M}_z = \hat{L}_z + 2 \cdot \hat{S}_z$ is the magnetic moment operator, and $Z = \sum_n \exp(-E_n/k_B T)$.

The measured susceptibility $\chi^{(z)}$ may be approximated as

$$\chi^{(z)} = \frac{\chi_{\text{CEF}}^{(z)}}{1 - \lambda \cdot \chi_{\text{CEF}}^{(z)}}, \quad (15)$$

where λ is the molecular field parameter. It should be noted that $\chi_{\text{CEF}}^{(z)}$ in Eq. (14) includes contributions from both Ce1 and Ce2 positions.

The least-squares fitting procedure was performed to approximate the experimental $\chi^{-1}(T)$ data using the relationship (15) (Fig. 8). The best result was obtained with $B_4^0(\text{Ce1}) = 0.06$ meV, $B_4^0(\text{Ce2}) = 0.10$ meV and $\lambda = 2.12$ mol/cm³. These CEF parameters correspond to energy splits $\Delta(\text{Ce1}) = 248$ K and $\Delta(\text{Ce2}) = 427$ K. The mean-field theory [26] offers the ordering temperature T_{ord} and the formula $T_{\text{ord}} = \lambda C$, where C is the Curie constant. The estimate of $T_{\text{ord}} \approx 2$ K can be obtained using the value of C from Table 2.

For $\text{Ce}_3\text{Pd}_{20}\text{Si}_6$, the low-temperature part of the

$\chi(T)$ curve is distorted by the magnetic transition (Figs. 3 and 4), which makes the CEF analysis more difficult. However, the rough approximation of $\chi(T)$ by Curie–Weiss law (Table 2) allows us to suggest that in $\text{Ce}_3\text{Pd}_{20}\text{Si}_6$ the CEF splitting of Ce^{3+} is weaker than in $\text{Ce}_3\text{Pd}_{20}\text{Ge}_6$. The thermal behavior of the electrical resistivity (Fig. 1) also supports this point of view.

4. Discussion

The results of this study allow us to suggest that the cerium compounds $\text{Ce}_3\text{Pd}_{20}\text{Si}_6$ and $\text{Ce}_3\text{Pd}_{20}\text{Ge}_6$ are new dense Kondo systems. Since the electrical resistivity ρ shows minima at different temperatures, i.e. at ~ 50 K for $\text{Ce}_3\text{Pd}_{20}\text{Si}_6$ and at ~ 10 K for $\text{Ce}_3\text{Pd}_{20}\text{Ge}_6$ (Fig. 1), the Kondo temperature T_K seems to be higher for the former compound. This could be due to the weaker CEF interaction in $\text{Ce}_3\text{Pd}_{20}\text{Si}_6$ than in $\text{Ce}_3\text{Pd}_{20}\text{Ge}_6$. The influence of the CEF splitting Δ on the effective Kondo temperature T_K was studied in Ref. [27]. For a cubic system with a Γ_7 ground state the relation between T_K and Δ was found to be

$$T_0^3 = T_K(T_K + \Delta)^2, \quad (16)$$

where T_0 is the Kondo temperature in the absence of CEF effects. If $\Delta \gg T_K$ then $T_K \approx T_0(T_0/\Delta)^2$. So, the effective Kondo temperature should decay rapidly with increasing Δ . This correlates with our conclusions about CEF effects in $\text{Ce}_3\text{Pd}_{20}\text{Si}_6$ and $\text{Ce}_3\text{Pd}_{20}\text{Ge}_6$.

We have found that the magnetic properties of $\text{Ce}_3\text{Pd}_{20}\text{Si}_6$ are very unusual. An antiferromagnetic-like transition was detected at ~ 50 K (Fig. 3), and below this temperature the magnetic moment versus the applied magnetic field demonstrates anomalous 'superparamagnetic' behavior (Fig. 5). It is important that the characteristic temperatures of Kondo and magnetic anomalies are close, in the region 50–60 K.

The assumption that two distinct Ce sublattices exist in the $\text{Ce}_3\text{Pd}_{20}\text{Si}_6$ system could help to explain most of the experimental data. Within the framework of this model, Ce2 atoms should interact, preferably inside 'small' cubes (Fig. 6). To a first approximation, this 'cube' can be considered as a 'molecule' with a magnetic moment that increases with decreas-

ing temperature (Fig. 7, inset). On cooling, the exchange interaction between the ‘molecules’ is enhanced and they can order antiferromagnetically. The Ruderman–Kittel–Kasuya–Yosida (RKKY) exchange interaction should be most important in $\text{Ln}_3\text{Pd}_{20}\text{X}_6$ compounds. Indeed, first, the minimum distance between Ce atoms is about 5 Å, and, second, Pd atoms are most numerous in the unit cell. From this point of view, other cerium positions (Ce1) should be less magnetically active because they have Ge or Si as nearest neighbors. In this scheme the Ce1 atoms may mostly play the role of Kondo scattering centers for the conduction electrons. Ordering in the Ce2 sublattice probably removes the magnetic Ce1–Ce2 interactions which are competitive with the Kondo ones. This could explain the enhanced increase in electrical resistivity after the magnetic transition in $\text{Ce}_3\text{Pd}_{20}\text{Si}_6$.

The coexistence of Kondo-like behavior and magnetic ordering may therefore be attributed to the relative isolation of two Ce subsystems. A similar situation occurs in high-temperature superconductors, in which antiferromagnetic ordering of the rare earth sublattice coexists with the superconductivity in copper–oxygen planes [28]. The different magnetic and transport properties of $\text{Ce}_3\text{Pd}_{20}\text{Si}_6$, $\text{Ce}_3\text{Pd}_{20}\text{Ge}_6$ may be partially due to the less marked distinction between the cerium positions in the latter compound [5]. The electron structure may also be strongly modified by atom replacement. This is clearly confirmed by the fact that the samarium and ytterbium homologues $\text{Sm}_3\text{Pd}_{20}\text{Si}_6$ and $\text{Yb}_3\text{Pd}_{20}\text{Si}_6$ display normal metallic and nonmagnetic behavior from 200 K down to 4.2 K.

Further experiments below 4.2 K, as well as specific heat measurements, are required for a better understanding of the magnetic and Kondo properties of $\text{Ln}_3\text{Pd}_{20}\text{X}_6$.

Acknowledgements

The authors wish to thank Dr A. Gribanov for the sample preparation and fruitful discussions. This work was supported by the Russian Fundamental Research Foundation (grant No. 95/02/04340) and the joint grant No. M78300 of the International Science Foundation and the Government of Russia.

References

- [1] N.B. Brandt and V.V. Moshchalkov, *Adv. Phys.* 33 (1984) 373.
- [2] Yu. Izumov, M. Katsnelson and Yu. Skryabin, *Itinerant Electron Magnetism* (Nauka, Moscow, 1994) p. 280.
- [3] S.Y. Mao, D. Jaccard, J. Sierro, Z. Fisk and J.L. Smith, *J. Magn. Magn. Mater.* 76–77 (1988) 241.
- [4] H. Yashima, *Solid State Commun.* 43 (1982) 595.
- [5] A.V. Gribanov, Yu.D. Seropegin and O.I. Bodak, *J. Alloys Comp.* 204 (1994) L9.
- [6] J.G. Sereni, G. Nieva, J.P. Kappler and P. Haen, *J. Physique I*, 1 (1991) 1499.
- [7] V.N. Nikiforov, J.M. Barakatova, Yu.D. Seropegin, Yu.V. Kochetkov, J. Mirković, M.V. Kovachikova, A.V. Gribanov and O.I. Bodak, 11th Int. Conf. on Solid Compounds of Transition Elements, Wrocław, 1994, P-79R(C) p. 90.
- [8] Yu.P. Gaidukov, Yu.A. Koksharov, Yu.V. Kochetkov, J. Mirković and V.N. Nikiforov, *Pis'ma v ZhETF* 61 (1995) 385.
- [9] J.B. Sousa, M.A. Amado, R.P. Pinto, M. Salgueiro Silva, M.E. Braga, B. Chevalier and J. Etourneau, *J. Magn. Magn. Mater.* 111 (1992) 239.
- [10] F. Lindeman, *Phys. Z.* 11 (1910) 609.
- [11] R.J. Elliott *Phys. Rev.* 94 (1954) 564.
- [12] S.V. Vonsovsky and M.S. Svirsky, *J. Appl. Phys.* 39 (1968) 649.
- [13] S.V. Vonsovsky, *Magnetism* (Nauka, Moscow, 1971) p. 386.
- [14] S.V. Vonsovsky, *Magnetism* (Nauka, Moscow, 1971) p. 713.
- [15] N. Oliveira, S. Foner, Y. Shapira et al., *Phys. Rev. B* 5 (1972) 2634.
- [16] G.B. Mardion, G. Vries, R. Tournier and R. Voyer, *C. R. Acad. Sci. Paris* 259 (1964) 4552.
- [17] E.L. Nagaev, *Magnetics with Complex Exchange Interactions* (Nauka, Moscow, 1988) p. 198.
- [18] C.P. Bean, *J. Appl. Phys.* 26 (1955) 1381.
- [19] V.L. Sedov, *Antiferromagnetism of γ -Fe: Invar Problem* (Nauka, Moscow, 1987) p. 73.
- [20] I.I. Sobelman, *Introduction to the Theory of Atomic Spectra* (Fizmatgiz, Moscow, 1963) p. 41.
- [21] L. Brillouin, *J. Phys. Radium* 8 (1927) 74.
- [22] J.C. Odo, *J. Phys. F: Metal Phys.* 13 (1983) 1291.
- [23] A. Abragam and B. Bleaney, *Electron Paramagnetic Resonance of Transition Ions* (Mir, Moscow, 1972) p. 162.
- [24] K.R. Lea, M.J.M. Leask and W.P. Wolf, *J. Phys. Chem. Solids* 23 (1962) 1381.
- [25] S.V. Vonsovsky, *Magnetism* (Nauka, Moscow, 1971) p. 111.
- [26] H.E. Stanley, *Introduction to Phase Transitions and Critical Phenomena* (Mir, Moscow, 1973) p. 137.
- [27] A. Okiji and N. Kawakami, *J. Magn. Magn. Mater.* 54–57 (1986) 327.
- [28] A.V. Narlikar, C.V. Narasimna Rao and S.K. Agarval, in: *Studies of High-Temperature Superconductors*, ed. A. Narlikar (Nova Science, New York, 1989) vol. 1, p. 341.